

Disorder–Order Ferroelectric Transition in the Metal Formate Framework of $[\text{NH}_4][\text{Zn}(\text{HCOO})_3]$

Guan-Cheng Xu, Xiao-Ming Ma, Li Zhang, Zhe-Ming Wang,* and Song Gao*

Beijing National Laboratory for Molecular Sciences, State Key Laboratory of Rare Earth Materials Chemistry and Applications, College of Chemistry and Molecular Engineering, Peking University, Beijing 100871, P. R. China

Received May 18, 2010; E-mail: zmw@pku.edu.cn; gaosong@pku.edu.cn

Abstract: A three-dimensional chiral metal formate framework compound, $[\text{NH}_4][\text{Zn}(\text{HCOO})_3]$, undergoes a paraelectric–ferroelectric phase transition at 191 K triggered by the disorder–order transition of NH_4^+ cations within the structure.

Ferroelectric materials are of importance and interest in both basic scientific concerns and versatile technological applications.^{1–3} The majorities are perovskite oxides^{1,2} such as BaTiO_3 and lead zirconate titanate (PZT); hydrogen-bonded inorganic salts such as Rochelle salt, potassium dihydrogen phosphate (KDP), and triglycine sulfate (TGS);¹ and recently reported organic ones.³ In the later classes, H bonding plays the key role in the electric ordering. The recently developed metal–organic frameworks (MOFs) have shown various properties or functionalities due to their hybrid inorganic–organic nature,⁴ but ferroelectric MOFs still remain scarce.^{5,6} Except for the symmetry requirement² for ferroelectrics, H-bonding systems can easily be created within MOFs if suitable components with H-bond donors and acceptors are chosen and properly organized in the solid state. Therefore, MOFs are promising candidates for ferroelectrics.^{4a,6a} On the other hand, the combination of the magnetism of MOFs with ferroelectricity should result in multiferroelectrics.^{6–9} In this context, we have systematically explored magnetic metal formate frameworks templated by protonated organic amines.⁷ Cheetham and other workers⁸ have shown that in our first-reported magnetic perovskite $[(\text{CH}_3)_2\text{NH}_2][\text{M}^{\text{II}}(\text{HCOO})_3]$ series⁹ the antiferroelectricity occurs in the 160–185 K range and that the disorder–order transition of the $(\text{CH}_3)_2\text{NH}_2^+$ template is the origin of electric ordering. We observed that the porous magnetic host framework of $[\text{Mn}_3(\text{HCOO})_6]$ with polar guests can lead to interesting dielectric properties, including ferroelectricity.¹⁰ These are new multiferroics. Very recently, we have found that the $[\text{NH}_4][\text{M}^{\text{II}}(\text{HCOO})_3]$ series¹¹ shows a structural phase transition in which the disordered NH_4^+ cation at room temperature (RT) becomes ordered at low temperature (LT). In this communication, we report that $[\text{NH}_4][\text{Zn}(\text{HCOO})_3]$ (**1**) shows a paraelectric–ferroelectric transition at the critical temperature $T_C = 191$ K, as characterized by single-crystal X-ray diffraction (XRD), dielectric anomaly, dielectric hysteresis loop, and preliminary thermodynamic studies, and we show that this is related to the disorder–order transition of the NH_4^+ cations within the structure.

1 was prepared by reaction of ammonium formate, formic acid, and $\text{Zn}(\text{ClO}_4) \cdot 6\text{H}_2\text{O}$ in methanol (see the Supporting Information). The bulk phase purity was verified by powder XRD (Figure S1 in the Supporting Information), and the material was thermally stable up to 100 °C (Figure S2). The slow diffusion method afforded hexagonal plate or bipyramidal crystals (Figure S3) up to 2 mm in size.

The structures of **1** at both 290 and 110 K were determined (Figure 1; also see Figure S4 and Tables S1 and S2). Here we focus on H-bonding systems and structural changes related to the ferroelectricity of **1**. At 290 K, the crystal belongs to the hexagonal space group $P6_322$, which has the nonpolar point group D_6 , with $a^{290\text{K}} = 7.3084(2)$ Å, $c^{290\text{K}} = 8.1705(3)$ Å, and $V^{290\text{K}} = 377.94(2)$ Å³. The crystal structure is the same as that of $[\text{NH}_4][\text{M}(\text{HCOO})_3]$ ($\text{M} = \text{Mn}^{2+}, \text{Co}^{2+}, \text{Ni}^{2+}$);^{11a} it features a three-dimensional chiral anionic $[\text{Zn}(\text{HCOO})_3]^-$ framework having a $(4^9 \cdot 6^6)$ network topology¹² (Figure 1a), with the arrays of NH_4^+ cations located in the framework's helical channels along the c direction (Figure S4a). Each octahedral Zn^{2+} node connects to six neighbors through anti–anti formate bridges. In the channel, the unique NH_4^+ cation shows disorder in a trigonal antiprism and forms $6 \times \frac{2}{3} = 4$ $\text{N} \cdots \text{H} \cdots \text{O}$ hydrogen bonds to the anionic framework, with a $\text{N} \cdots \text{O}$ distance of 2.972 Å and a $\text{N} \cdots \text{H} \cdots \text{O}$ angle of 161° (Figure 1b). The disorder of the NH_4^+ indicates the competition among different H-bonding sites at room temperature. Disorder of protonated ammine cations has been observed for many metal formate compounds.^{7–9,11,13}

1 was observed to undergo a structural phase transition at ~190 K, accompanied by the tripling of the unit cell, the disorder–order transition of NH_4^+ with related structure changes (Figure 1 and Figures S4b and S5), and a change in space group from $P6_322$ to the polar $P6_3$. The length of $c^{110\text{K}}$ axis, 8.2015(2) Å, is slightly longer than $c^{290\text{K}}$, while $a^{110\text{K}}$ becomes the diagonal $(a-b)^{290\text{K}}$ of the $(ab)^{290\text{K}}$ rhombus, whose length of 12.5919(3) Å is very close to $3^{1/2}a^{290\text{K}}$; therefore, $V^{110\text{K}} = 1126.18(5)$ Å³, which is almost equal to $3V^{290\text{K}}$. The tripling of the unit cell at 110 K was also evidenced by the observation of weak diffraction spots in the oscillation image at 110 K that were not observed at 290 K (Figure S5). Thus, the unique channel at $(0, 0, z)$ in the 290 K structure was split into three unique channels at $(0, 0, z)$, $(\frac{2}{3}, \frac{1}{3}, z)$, and $(\frac{1}{3}, \frac{2}{3}, z)$, locating three unique, ordered, tetrahedral NH_4^+ cations, each with one apical and three basal N–H groups. Each basal N–H group forms a stronger H bond to the metal formate framework, with $\text{N} \cdots \text{O}$ distances of 2.830–2.864 Å and $\text{N} \cdots \text{H} \cdots \text{O}$ angles of 167–175°. The apical N–H group, with the N–H directing c axis, still forms a trifurcated acceptor-type H bond,¹⁴ with $\text{N} \cdots \text{O}$ distances of 3.075–3.120 Å and $\text{N} \cdots \text{H} \cdots \text{O}$ angles of 103–105°. It is noted that within the unit cell, the NH_4^+ cations in the channels at $(\frac{2}{3}, \frac{1}{3}, z)$ and $(\frac{1}{3}, \frac{2}{3}, z)$ have their apical N–H groups pointing in the $+c$ direction, but the NH_4^+ cations in the channel at $(0, 0, z)$ have the apical N–H groups pointing in the opposite direction. More importantly, the N atoms of the NH_4^+ cations in the three channels are shifted by -0.36 , -0.38 , and $+0.40$ Å along the c direction with respect to the anionic framework compared to the zero shift in the 290 K structure, which has a zero shift (Figure S4); this indicates the double potential wells for the NH_4^+ cations in the channel. These are related to the polar LT structure and the observed

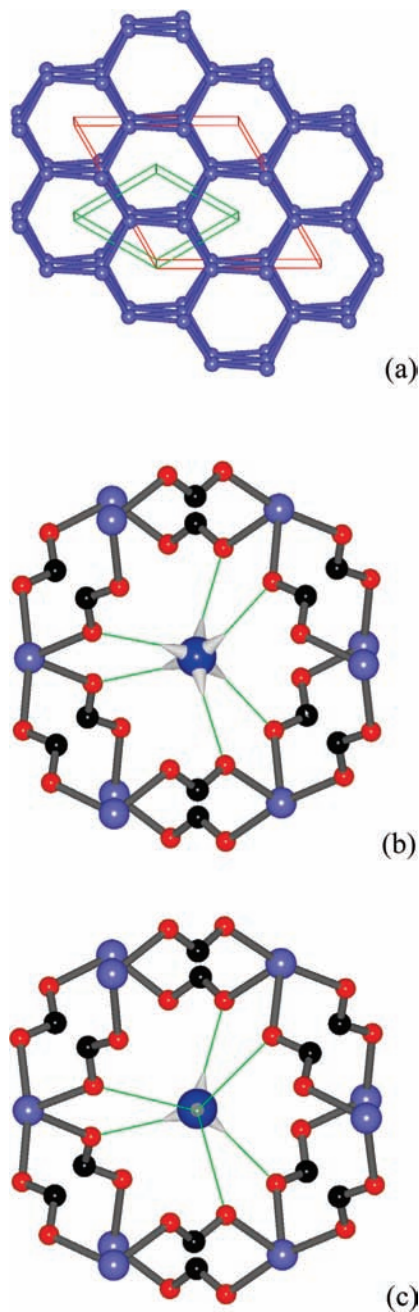


Figure 1. (a) Topological view of the $(4^9 \cdot 6^6)$ anionic framework in **1**; spheres are Zn^{2+} and sticks HCOO^- . Green and red boxes are unit cells at 290 and 110 K, respectively. (b) One trigonally disordered NH_4^+ cation in the channel at 290 K. (c) One ordered NH_4^+ tetrahedral cation in the channel at 110 K. All views are along the c axis. Atom scheme: H, white; C, black; O, red; Zn, blue-violet; N, blue. In (b) and (c), thin green lines are $\text{N-H} \cdots \text{O}$ hydrogen bonds; H atoms of formate have been omitted.

ferroelectricity. The C_6 point group of the LT phase is a subgroup of the D_6 point group of the RT phase in which the twofold axes have vanished, indicating the symmetry breaking and coinciding with a typical ferroelectric type of 622F6 in the Aizu notation.¹⁵

The temperature dependence of the dielectric permittivity (ϵ) of **1** was measured on a single crystal of **1** (Figure S3) under an applied electric field $E \parallel c$ with frequencies of 100 Hz to 1 MHz. Indeed, the real component, ϵ' , showed very high dielectric anomaly peaks at 191–192 K (Figure 2a), corresponding to the transition. The peak ϵ' values are several or tens-fold larger than those at higher and lower temperatures. This is characteristic of a ferroelectric

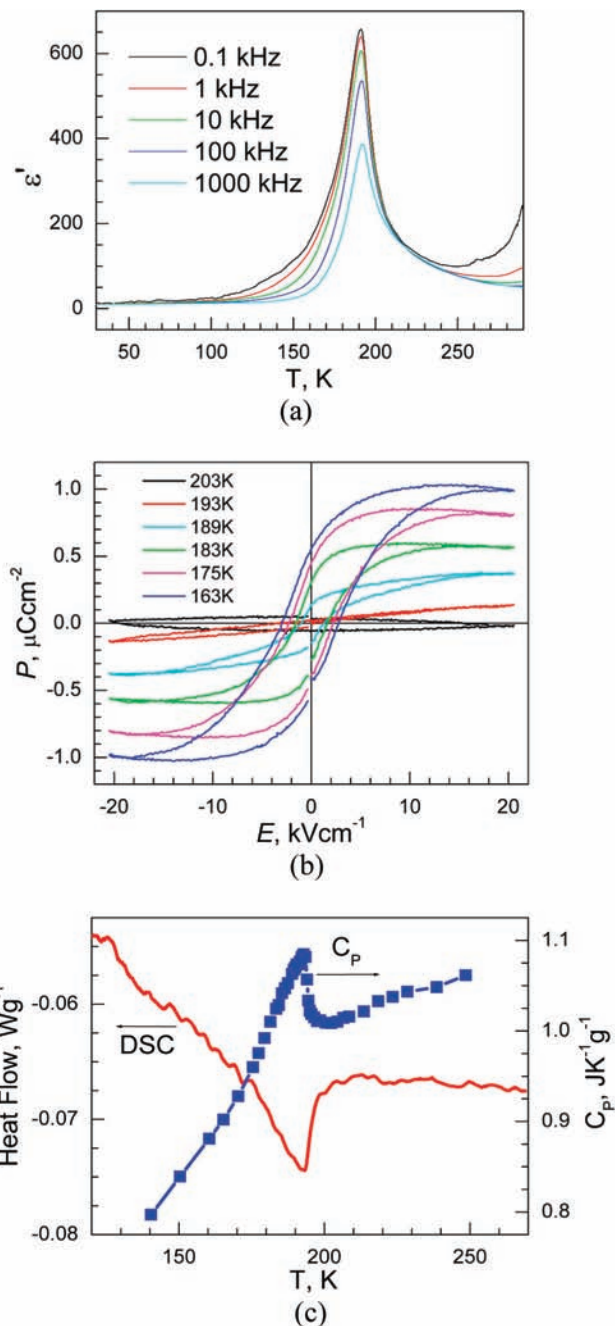


Figure 2. (a) Temperature-dependence of the dielectric permittivity ϵ' of **1**, with $E \parallel c$. (b) Dielectric hysteresis loops of **1** with $E \parallel c$ at various temperatures. (c) DSC and C_p plots for **1**.

transition. The reciprocal ϵ' data at 10 kHz between 210 and 260 K fitted the Curie–Weiss law well (Figure S6), affording the Curie constant $C = 5.39 \times 10^3$ K and the Curie–Weiss temperature $T_0 = 181$ K. The C value is comparable to those of ferroelectrics undergoing disorder–order transitions of H-bonding systems, such as KDP and TGS,^{1,3} and T_0 is slightly lower than $T_C = 191$ K.

The ferroelectricity was confirmed by the dielectric hysteresis loops of polarization measured with $E \parallel c$ below T_C (Figure 2b). The characteristic loop clearly occurred at 189 K, just below T_C . The spontaneous polarization increased on cooling and reached saturation at 163 K with a remnant polarization (P_r) of $0.68 \mu\text{C cm}^{-2}$, a coercive field (E_c) of 2.8 kV cm^{-1} , and a saturation spontaneous polarization (P_s) of $1.03 \mu\text{C cm}^{-2}$, all of which are typical for H-bonded ferroelectrics.^{1,3} In the LT phase, the shifts

of NH_4^+ cations related to the anionic framework could be considered to create dipoles with \pm unit charges separated by these shifts along the c axis, from which P_s could be easily estimated as $0.96 \mu\text{C cm}^{-2}$, in agreement with the above experimental value.

1 was subjected preliminary differential scanning calorimetry (DSC) and specific heat (C_p) measurements (both in heating mode; Figure 2c). An endothermic peak in the DSC curve and a λ -shaped peak in the C_p data were clearly observed at 192 K, corresponding to the paraelectric–ferroelectric transition. The ΔH and ΔS were estimated as $\sim 0.7 \text{ kJ mol}^{-1}$ and $\sim 2 \text{ J mol}^{-1} \text{ K}^{-1}$, respectively. From the Boltzmann equation, $\Delta S = R \ln N$, where R is the gas constant and N is the ratio of the numbers of respective geometrically distinguishable orientations, we obtain $N = 1.3$. This value is less than the value $N = 2$ denoting two discrete states in the disorder phase, indicating the discomplicated disordered–ordered feature of the phase transition.^{8a,b} These results confirm the phase transition, though the thermodynamic characteristics need further investigation.

In conclusion, the paraelectric–ferroelectric phase transition at 191 K triggered by the disorder–order transition of NH_4^+ cations in the metal formate framework of **1** has successfully been established. As a large number of magnetic metal formate frameworks templated by various protonated amines have been discovered,^{7–9,11,13} the finding of ferroelectricity in **1** opens an avenue to a new class of MOF-based multiferroics, and this research is underway.

Acknowledgment. This work was supported by the NSFC (Grants 20871007 and 20821091), the National Basic Research Program of China (Grants 2006CB601102 and 2009CB929403), and the China Postdoctoral Science Foundation (Grant 20090450232). We thank Prof. Dr. Wen Zhang, Prof. Dr. Hong-Ling Cai, and Prof. Dr. Ren-Gen Xiong of Southeast University, China, for their kind help with the dielectric and ferroelectric measurements and valuable discussions.

Supporting Information Available: Experimental details, Tables S1 and S2, Figures S1–S6, and CIF files for the two structures in this

communication. This material is available free of charge via the Internet at <http://pubs.acs.org>.

References

- (1) (a) Lines, M. E.; Glass, A. M. *Principles and Applications of Ferroelectrics and Related Materials*; Clarendon Press: Oxford, U.K., 1977. (b) Jona, F.; Shirane, G. *Ferroelectric Crystals*; Pergamon Press: Oxford, U.K., 1962.
- (2) (a) Ahn, C. H.; Rabe, K. M.; Triscone, J.-M. *Science* **2004**, *303*, 488. (b) Haertling, G. H. *J. Am. Ceram. Soc.* **1999**, *82*, 797. (c) Scott, J. F. *Science* **2007**, *315*, 954.
- (3) (a) Horiuchi, S.; Tokunaga, Y.; Giovannetti, G.; Picozzi, S.; Itoh, H.; Shimano, R.; Kumai, R.; Tokura, Y. *Nature* **2010**, *463*, 789. (b) Horiuchi, S.; Tokura, Y. *Nat. Mater.* **2008**, *7*, 357. (c) Horiuchi, S.; Kumai, R.; Tokura, Y. *Angew. Chem., Int. Ed.* **2007**, *46*, 3497. (d) Horiuchi, S.; Kumai, R.; Tokunaga, Y.; Tokura, Y. *J. Am. Chem. Soc.* **2008**, *130*, 13382.
- (4) (a) Cheetham, A. K.; Rao, C. N. R. *Science* **2007**, *318*, 58. (b) Long, J. R.; Yaghi, O. M. *Chem. Soc. Rev.* **2009**, *38*, 1213. (c) Kepert, C. J. *Chem. Commun.* **2006**, 695. (d) Reed, C. A. *Acc. Chem. Res.* **2005**, *38*, 215. (e) Kitagawa, S.; Kitaura, R.; Noro, S. *Angew. Chem., Int. Ed.* **2004**, *43*, 2334.
- (5) (a) Zhang, W.; Xiong, R. G.; Huang, S. D. *J. Am. Chem. Soc.* **2008**, *130*, 10468. (b) Guo, Z. G.; Cao, R.; Wang, X.; Li, H. F.; Yuan, W. B.; Wang, G. J.; Wu, H. H.; Li, J. J. *J. Am. Chem. Soc.* **2009**, *131*, 6894.
- (6) (a) Ohkoshi, S.; Tokoro, H.; Matsuda, T.; Takahashi, H.; Irie, H.; Hashimoto, K. *Angew. Chem., Int. Ed.* **2007**, *46*, 3238. (b) Rogez, G.; Viart, N.; Drillon, M. *Angew. Chem., Int. Ed.* **2010**, *49*, 1921.
- (7) (a) Wang, Z. M.; Hu, K. L.; Gao, S.; Kobayashi, H. *Adv. Mater.* **2010**, *22*, 1526. (b) Wang, X. Y.; Wang, Z. M.; Gao, S. *Chem. Commun.* **2008**, 281.
- (8) (a) Jain, P.; Ramachandran, V.; Clark, R. J.; Zhou, H. D.; Toby, B. H.; Dalal, N. S.; Kroto, H. W.; Cheetham, A. K. *J. Am. Chem. Soc.* **2009**, *131*, 13625. (b) Jain, P.; Dalal, N. S.; Toby, B. H.; Kroto, H. W.; Cheetham, A. K. *J. Am. Chem. Soc.* **2008**, *130*, 10450. (c) Sánchez-Andújar, M.; Presedo, S.; Yáñez-Vilar, S.; Castro-García, S.; Shamir, J.; Señaris-Rodríguez, M. A. *Inorg. Chem.* **2010**, *49*, 1510.
- (9) (a) Wang, Z. M.; Zhang, B.; Otsuka, T.; Inoue, K.; Kobayashi, H.; Kurmoo, M. *Dalton Trans.* **2004**, 2209. (b) Wang, X. Y.; Gan, L.; Zhang, S. W.; Gao, S. *Inorg. Chem.* **2004**, *43*, 4615.
- (10) (a) Cui, H. B.; Takahashi, K.; Okano, Y.; Kobayashi, H.; Wang, Z. M.; Kobayashi, A. *Angew. Chem., Int. Ed.* **2005**, *44*, 6508. (b) Cui, H. B.; Wang, Z. M.; Takahashi, K.; Okano, Y.; Kobayashi, H.; Kobayashi, A. *J. Am. Chem. Soc.* **2006**, *128*, 15074.
- (11) (a) Wang, Z. M.; Zhang, B.; Inoue, K.; Fujiwara, H.; Otsuka, T.; Kobayashi, H.; Kurmoo, M. *Inorg. Chem.* **2007**, *46*, 437. (b) Ma, X. M. B.Sc. Thesis, Peking University, Beijing, China, 2009. (c) Xu, G. C.; Zhang, L.; Wang, Z. M.; Gao, S. The Second Asian Conference on Coordination Chemistry, Nanjing, China, November 2009.
- (12) Batten, S. R.; Robson, R. *Angew. Chem., Int. Ed.* **1998**, *37*, 1460.
- (13) (a) Wang, Z. M.; Zhang, X. Y.; Batten, S. R.; Kurmoo, M.; Gao, S. *Inorg. Chem.* **2007**, *46*, 8439. (b) Hu, K. L.; Kurmoo, M.; Wang, Z. M.; Gao, S. *Chem.—Eur. J.* **2009**, *15*, 12050.
- (14) Desiraju, G. R.; Steiner, T. *The Weak Hydrogen Bond in Structural Chemistry and Biology*; Oxford University Press: New York, 1999.
- (15) Aizu, K. *Phys. Rev.* **1966**, *146*, 423.

JA104263M